# Lagrangian Wind and Current Vectors Very Close to a Short-Fetch Wind-Swept Surface[1]

ALLEN H. SCHOOLEY

*Ocean Sciences Division, Naval Research Laboratory, Washington, DC 20375*

29 January 1979 and 23 March 1979

ABSTRACT

Drag used in aeronautics and wind stress used in oceanography are essentially equivalent under short-fetch conditions, where the wind velocity substantially exceeds the water velocity. Likewise, lift and wave height are related under the same conditions.

An average short fetch wind velocity of 10 m $s^{-1}$ shows the properties of increasing drag and lift from the trough to the skewed downwind peak. Immediately after the peak the drag and lift drop to a low value corresponding to a region of aerodynamic stall. Recovery is rapid and the process is repeated for the next wave.

In spite of the similarities, short-fetch water waves are not well designed air foils. They are somewhat like flying an airfoil backward.

## 1. Introduction

Many meteorological and oceanographic measurements are obtained from fixed points in space known as the Eulerian reference method. The Lagrangian reference system involves following a multiplicity of single, substantially neutrally-buoyant particles as they move through the air, the water and along the air-water interface. Lagrangian measurements are more difficult to obtain but the results are usually more easily visualized (Munn, 1966).

When there is interest in short-fetch air-flow and wind-forced water flow, at or within a few millimeters of the undulating naviface (Montgomery, 1969), Lagrangian measurements are helpful.

## 2. Laboratory experiments

The heavy line across the center of Fig. 1 is an average short-fetch wind-wave profile produced in a water-wind tunnel by a 10 m $s^{-1}$ wind measured 5 cm above the mean naviface. The wave crest is skewed downwind and the average wavelength is 12 cm. The average elapsed time of the wave past point zero was approximately 0.3 s. The wave trough to wave height averaged about 0.8 cm. Waves of this type are often seen as the finestructure superimposed on longer and larger waves at sea. Their effect cannot be neglected (Stewart, 1969; Phillips, 1977).

In Fig. 1 the numbers along the average wave profile show the measured mean surface water drift velocity (cm $s^{-1}$) along the wave surface using thin beeswax floats (Schooley, 1963). The highest surface velocities are just after the crest and the lowest velocity just before the trough. This water wave was formed and maintained by the wind field in the short-fetch water-wind tunnel. The trajectories of many small helium-filled neutrally-buoyant soap bubbles were traced by high-speed cinematography to determine the average magnitude, direction and standard deviation of the wind vectors above the water (Schooley, 1963). A 10 m $s^{-1}$ calibration of the horizontal and vertical wind vector scales is shown in the upper right corner of Fig. 1.

Subsurface trajectories of many random clumps of especially prepared aluminum flakes were traced by novel cinematography to determine the magnitude, direction and standard deviation of the water flow at several places beneath the surface to a depth of about 5 mm. These subsurface vectors show that there are relatively large changes in vector magnitude, direction and standard deviation between the crest and the trough. In the trough region the average wave profile line is only approximately representative of the actual situation. From time to time there were small droplets of water that blew off the crest of the wave and then fell back into the water in front of the crest. This indicates that there were wind eddies in this region (Jeffreys, 1925).

The 10 cm $s^{-1}$ subsurface vertical and horizontal vector scales are at the lower left of Fig. 1. The much slower flow and much greater density of the water compared to the air results in the water surface approximating the top of a solid airfoil where drag (wind stress) and lift may be calculated.

[1] Presented at the XVI General Assembly IUGG, Grenoble, France, 25 August–6 September, 1975.

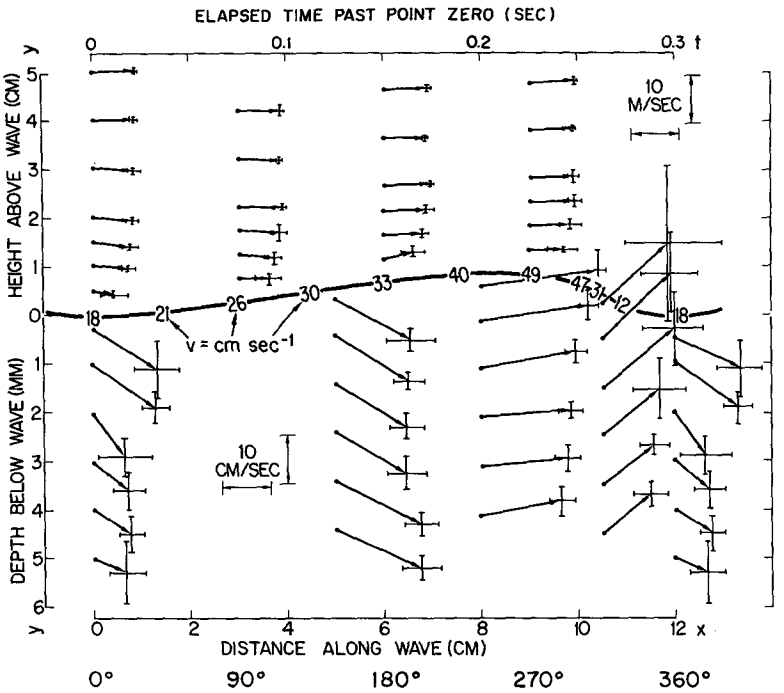


FIG. 1. Experimentally determined wind and current vectors together with the surface velocities associated with similar short-fetch, high-velocity, wind-driven water waves.

## 3. Vector diagrams

The air and the water Cartesian vectors of Fig. 1 may be transformed to circular polar coordinate form as shown in Figs. 2 and 3.

In Fig. 2 the wind velocity vectors at the wave surface and at 0.5 and 2 cm above are displayed. One wavelength starts at 0° and makes one full rotation through 90°, 180°, 270° and back to 360° = 0°.

In Fig. 3 the average rotating vectors in the relative slow velocity water 0.5 and 5 mm below the surface are shown. They are distorted by the skew-

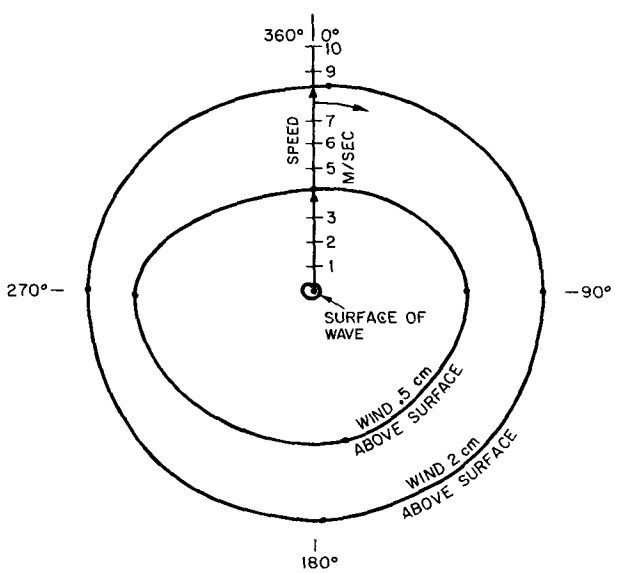


FIG. 2. Wind Cartesian vectors of Fig. 1 transformed to polar coordinate form.

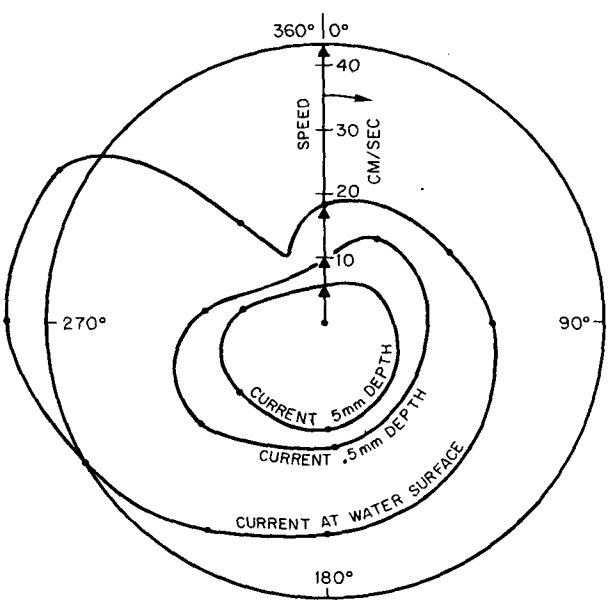


FIG. 3. Average rotating vectors in the water.

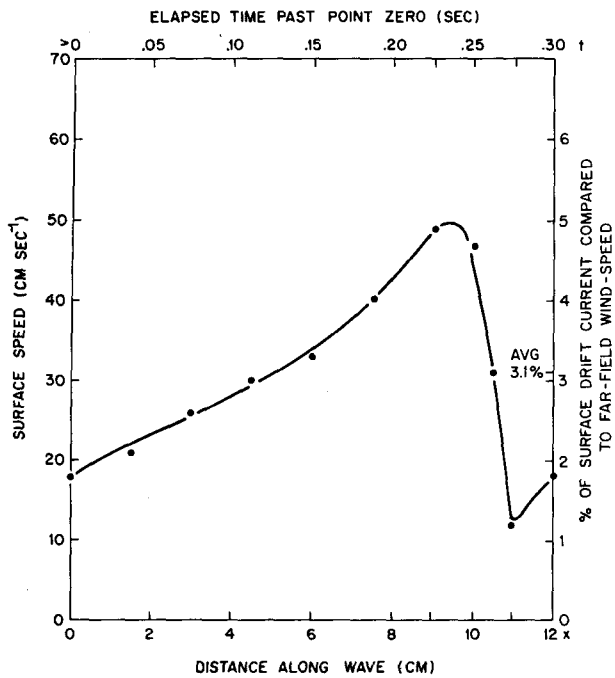


FIG. 4. Vertical expansion of surface velocities along the wave that were noted numerically in Fig. 1.

ness and turbulence of the surface water. It is estimated from inspection of this figure that the friction layer below the wind surface is on the order of about 0.1 cm thick with an equivalent mass per unit area of surface of $m = 0.1$ g cm$^{-2}$. This is obviously a rough approximation.

In Fig. 4 the bottom horizontal scale represents the distance along the average wave shown in Fig. 1. The upper horizontal scale represents the approximate elapsed time of the wave past point zero. The left scale is the measured surface drift speed along the wave. The dimensionless scale on the right is the percent of the surface drift current compared to the far-field wind speed of 10 m s$^{-1}$. The surface drift current average is 3.1% in the short-fetch water-wind tunnel. This compares with an average of 2.4% from the compilation of 16 sea investigations reported by James (1966).

The curve of Fig. 4 was graphically differentiated to yield near-surface acceleration $a = \Delta v/\Delta t$ [cm s$^{-2}$] along the wave. If the effective surface unit mass $m$ is 0.1 g cm$^{-2}$ as previously assumed, $ma = 0.1a$ = surface drag or tangential force in dynes per square centimeter.

Shemdin (1972) points out that wind action over water generates both waves and surface drift and the transfer of momentum and energy from the air to water by normal and tangential stresses is not completely understood. His work indicates that the average tangential stress along a wave with a far-field wind of 10 m s$^{-1}$ was measured to be about $\tau_s = 2.7$ dyn cm$^{-2}$. Shemdin's tangential stress figure is an average along a short-fetch water wave that was simultaneously disturbed mechanically, and by the wind.

Reisbig *et al.* (1973) noted that in light of their experimental study, it appeared that the surface shear stress fluctuates over the surface of the water wave and may result in part from the separated turbulent air flow in the wave trough. The work herein described confirms this conclusion.

Jeffrey's (1925) hypotheses of sheltering and skin friction, though discounted for many years for large ocean waves, appear to be conceptually correct for short-fetch waves under strong wind conditions.

In Fig. 5, the bottom horizontal scale represents the distance along the average water wave shown in Fig. 1. The height of the wave with respect to the trough is expanded by a factor of approximately 10 and translated to zero average height as indicated by the scale on the left.

With no wind blowing the water would be calm at the zero level. With the wind blowing, much of the momentum goes into depressing and lifting water waves as well as producing tangential drag currents (Stewart, 1969).

Usually the lift and drag along a wave cannot be separated, as is commonly done with airfoils. However, for short waves produced by rather strong winds the separation is possible and the results for such a case are interesting.

## 4. Definition of terms and assumptions

$x$ distance along wave (cm)
$v$ surface drift speed along wave (cm s$^{-1}$)
$t$ elapsed time of wave past point zero (s)

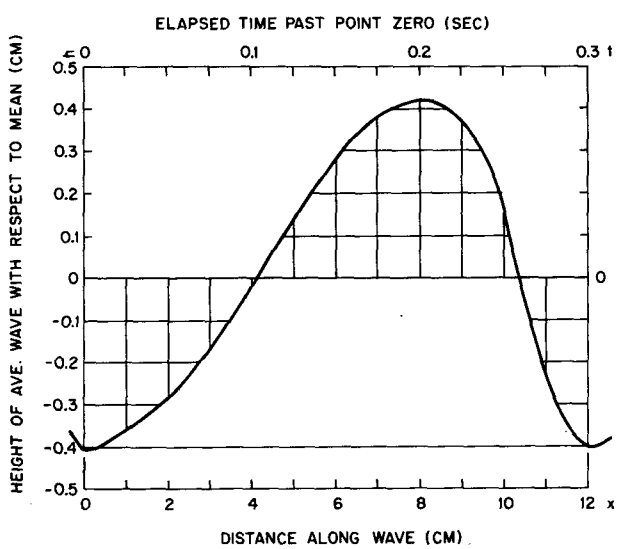


FIG. 5. Time and/or distance variation of wave height. If there was no wind, the water would be flat and smooth at zero mean height. Wind exerts regions of lift and depression as the wave forms in the Lagrangian time frame.

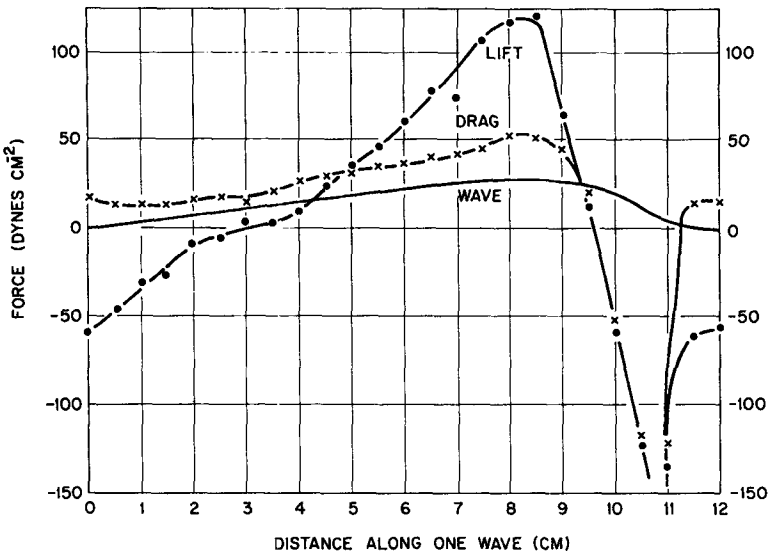


FIG. 6. Drag (wind stress) and lift peak near the peak of the wave. A sharp drop occurs in the turbulent region after the peak. Recovery occurs near the trough.

$a = \Delta v/\Delta t$ surface acceleration along wave (cm s$^{-2}$)

$m$ effective surface mass density along water wave; assumed to be (1 g cm$^{-3}$) (0.1 cm depth) = 0.1 g cm$^{-2}$

$D = ma$ horizontal drag force density or wind stress along wave (dyn cm$^{-2}$)

$L$ lift force along wave is ± weight of a unit area column of water along $x$, with respect to mean height of wave (dyn cm$^{-2}$) (refer to Fig. 5).

## 5. Conclusion

The previous paragraph is a summary of the measurements, assumptions and calculations of lift and drag along an average short-fetch wave. The results are shown in Fig. 6. (The wave shape in Fig. 6 is drawn in merely as a reference. Its real vertical scale is shown in Fig. 1.) Fig. 6 indicates that there is low drag and negative lift at 0 cm along the wave. They both are positive and are increasing at 5 cm. The drag is highest and the lift spectacularly high at 8 cm. At 10 cm both are falling fast between about 10.75 and 11 cm. At 12 cm both have recovered to the values at 0 cm.

For the first 8 cm the curves behave more or less like a normal aeroplane wing. Between 8 and 11 cm the situation is more like a wing in a serious turbulent stall.

## REFERENCES

James, R. W., 1966: Ocean thermal structures forecasting. Gov't. Printing Office, Washington, DC, 37 pp.

Jeffreys, G. I., 1925: On the formation of water waves by the wind. *Proc. Roy. Soc. London*, **A107**, 189–206.

Montgomery, R. B., 1969: The words naviface and oxyty. *J. Mar. Res.*, **27**, 161–162.

Munn, R. E., 1966: *Descriptive Micrometeorology*. Academic Press, 37 pp.

Phillips, O. M., 1977: The surface of the sea. *ONR Nav. Res. Rev.*, May, 19–28.

Reisbig, R. L., Alofs, D. J., Shah, R. C., and Banerjee, S. K., 1973: Measurements of oil spill-drift caused by the coupled parallel effects of wind and waves. *Mem. Soc. Roy. Sci. Liege*, **6**, No. 6, 67–77.

Schooley, A. H., 1963: Simple tools for measuring wind fields above wind-generated water waves. *J. Geophy. Res.*, **63**, 5497–5504.

Shemdin, O. H., 1972: Wind-generated current and phase speed of windwaves. *J. Phys. Oceanogr.*, **2**, 411–419.

Stewart, R. W., 1969: The ocean. *Sci. Amer.*, 27–38.